IJE TRANSACTIONS C: Aspects Vol. 26, No. 12, (December 2013) 1433-1444

International Journal of Engineering

Journal Homepage: www.ije.ir

Crack Detection of Timoshenko Beams Using Vibration Behavior and Neural Network

M. Rakideh, M. Dardel, M. H. Pashaei *

Babol Noshirvani University of Technology, Department of Mechanical Engineering, Babol, Iran

PAPER INFO

Paper history:
Received 27 January 2013
Received in revised form 12 March 2013
Accepted 18 April 2013

Keywords:
Crack Detection
Timoshenko Beam
Neural Network

ABSTRACT

In this research, at first, natural frequencies of a cracked beam are obtained analytically. Also, the location and the depth of a crack in the beam are identified by neural network method, in this study. This research is applied on a beam with an open edge crack for three different boundary conditions. For this purpose, firstly, the natural frequencies of the cracked beam are analytically obtained to get the examples for training the neural network. Then, inversely, the trained neural network is used for obtaining the location and depth of the crack. The effect of the numbers of the natural frequencies as input of the network was evaluated on the prediction accuracy. Results and measure of errors show that the neural network is a powerful method to determine the location and depth of crack. Also, increasing the numbers of the natural frequencies causes the prediction accuracy to be increased.

doi: *10.5829/idosi.ije.2013.26.12c.04*

1. INTRODUCTION

The study of the damage of the structures is an important prospect to evaluate structural systems in order to ensure their safety. Some structures such as large bridges are required to be continuously considered to detect possible damages (e.g., cracks) to make sure about the uninterrupted service. Finding out the crack location and depth has been identified as an "inverse problem". Nowadays, cracks are generally being detected by non-destructive testing methods (e.g., ultrasonic testing, X-ray, etc.). These methods are costly and time consuming specially for long components such as railway tracks and pipelines [1]. As a result, the analytical and numerical methods are being developed to determine the location and depth of the crack. These methods make the cost and time to be reduced.

There are two general solutions for finding out the crack location and depth. The first one is involved with using of the natural frequencies whereas, other one is based on the dynamic response (applying the load and then finding out the crack location and depth, afterwards). In most cases, an auxiliary method is applied with the methods. For the purpose of finding out the crack location and depth, Taghi et al. have used the genetic algorithm [2]. Nahvi and Jabbari determined the location and depth of the crack using finite element method and have confirmed it by modal test [3] Nandwana and Maiti have used the natural frequencies for the same purpose as preceding researches [4]. Zhong and Oyadiji used stationary wavelet transform to find out crack location and depth [5]. Rrzos and Aspragathos performed it by vibration modes [6]. In this research, crack location and depth is achieved using natural frequencies and neural network.

A number of methods can be found to model the cracked section. One of these methods uses the reduced section modulus of the cracked section as a model [7], while another one tries to estimate a local flexibility for cracked sections [8]. Replacing cracked section by a rotational spring is another method in which shear effect in bending has been neglected [9–11]. In this research, the crack is modeled as a rotational spring.

In most previous studies the Euler– Bernoulli theory has been used, neglecting the effect of shear deformations. This theory has been applied to the cracked beams with different boundary conditions. Lele

*Corresponding Author Email: mpashaei@nit.ac.ir (M. H. Pashei)

and Maiti [12] proposed a new method based on Timoshenko beam theory considering shear effects. In that research, the characteristic equation for the cantilever cracked beam is derived. In this research, Timoshenko beam theory has been used, since the Euler-Bernouli theory is suitable for height to length ratio under 0.1.

This study starts with analytical determination of the natural frequencies of Timoshenko beams including an open crack. It follows with a brief description of the Back-propagation neural network. The neural network will be trained by analytically obtained natural frequencies, afterwards. In the next step, the trained neural network is used to obtain the location and depth of the crack. Examinations of the trained neural network for different non-trained cases are presented. The effect of numbers of natural frequencies as input of the network is evaluated on the prediction accuracy. The proposed method is general and can be applied to any structure with any number of cracks. Finally, the uniqueness of the identification of the depth and location of the crack by neural network is discussed.

Free and forced vibration analysis of a cracked beam was performed by Orhan [13] in order to identify the crack in a cantilever beam. Single- and two-edge cracks were evaluated. It has been cleared by the results that the free vibration analysis provides suitable information relating to the detection of the single and two cracks, whereas forced vibration can detect only the single crack condition. However, dynamic response of the forced vibration describes the changes in the crack depth and location better than the free vibration, since, the differences among the natural frequencies corresponding to a change in the crack depth and location has a minor effect on the free vibration. An analytical approach to evaluate the forced vibration response of the uniform Timoshenko beams with an arbitrary number of open edge cracks which is excited by a concentrated moving load is developed by Shafiei and Khaji [14]. For this purpose, the cracked beam is modeled using beam segments connected by rotational springs. These springs are assumed to be massless, linear elastic with sectional flexibility. An analytical approach for crack identification procedure in uniform beams with an open edge crack, based on bending vibration measurements is developed by Khaji et al. [15].The cracked beam is modeled as two segments connected by a rotational massless linear elastic spring with sectional flexibility. The Timoshenko beam theory has been used to model each segment of the continuous beam. Dynamic response of the functionally graded Timoshenko beams with an open edge crack resting on an elastic foundation subjected to a transverse load moving at a constant speed has been studied by Yan et al. [16]. It is assumed that the material properties follow an exponential variation through the thickness of the beam. The cracked beam is modeled as an assembly of two sub-beams connected through a linear rotational spring. Free vibration analysis of an elastically supported cracked beam is investigated by Matbuly et al. [17]. The beam is made of a functionally graded material and rested on a Winkler–Pasternak foundation. The linear spring model is employed to formulate the problem and method of differential quadrature is applied to solve the problem. The vibration of non-uniform rectangular beams in the bending mode with multiple edge cracks along the beam's height is investigated by Mazanoglu and Sabuncu [18]. The energy based method is used for defining the vibration of the beam with cracks along its height.

Crack detection in beam structures based on kurtosis is presented by Hadjileontiadis et al. [19]. The fundamental vibration mode of the cracked cantilever beam is analyzed and both the location and size of the crack are estimated. The location of the crack is determined by the abrupt changes in the spatial variation of the analyzed response, while the size of the crack is related to the estimate of kurtosis. Crack identification in the beam structures based on wavelet analysis is presented by Douka et al. [20]. The fundamental vibration mode of a cracked cantilever beam is analyzed using continuous wavelet transform and both the location and size of the crack are estimated. The position of the crack is located by the sudden change in the spatial variation of the transformed response. To estimate the size of the crack, an intensity factor is defined which relates the size of the crack to the coefficients of the wavelet transform. A two-step approach based on the mode shape curvature and response sensitivity analysis for crack identification in the beam structures is presented by Lu et al. [21]. The location of the crack is identified from a modified difference between the mode shape curvatures of the cracked and intact beams in the first step. A response sensitivity based on the model updating method is utilized to identify the location and depth of the crack precisely, in the second step. Analytical approach to investigate natural frequencies and mode shapes of a stepped beam with an arbitrary number of transverse cracks and general form of boundary conditions is presented by Attar [22]. Also, an inverse problem of determining the location and depth of multiple cracks is given.

In this work, identification of the depth and location of the crack in a beam is carried out using neural network method. For this purpose, at first an analytical method is presented to obtain natural frequency of the cracked Timoshenko beam. The obtained data are used to design a neural network. The location and depth of cracks for non-learn data of neural network is examined to show the applicability of the presented method, finally.

2. MATHEMATICAL MODEL

Consider an elastic cracked Timoshenko beam of length L, uniform cross-section area A and moment of inertia I, with a crack at position of eL as shown in Figure 1. The crack can be modelled as a massless torsional spring with stiffness K_c. The strain and kinetic energies and the work of rotational spring with stiffness K_c for Timoshenko beam with open crack can be determined as follows [23]:

$$\boldsymbol{V}=\frac{1}{2}\int_0^l\left[EI(x)\left(\frac{\partial\psi}{\partial x}\right)^2+kAG\left(\frac{\partial w}{\partial x}-\psi\right)^2\right]dx \tag{1}$$

$$\boldsymbol{T}=\frac{1}{2}\int_0^l\left[\rho A(x)\left(\frac{\partial w}{\partial t}\right)^2+\rho I\left(\frac{\partial\psi}{\partial t}\right)^2\right]dx \tag{2}$$

$$\boldsymbol{W}=-K_c\left(\left.\frac{\partial w}{\partial x}\right|_{e^+}-\left.\frac{\partial w}{\partial x}\right|_{e^-}\right)\psi(x,t) \tag{3}$$

where $w(x,t)$ is the transverse deflection and $\psi(x,t)$ is the slope of the deflection curve due to the bending. E, G and ρ indicate the Young's modulus, the shear modulus and mass density per unit lenght, respectively. k represents the shear correction factor and is assumed to be 5/6.

It is assumed that crack is located at the distance e from left end of the beam. Dividing beam into two segments and applying the extended Hamilton principle to Equations (1) and (2) gives:

$$\begin{aligned}\int_{t_1}^{t_2}\Bigg\{&-EI\frac{\partial\phi}{\partial x}\delta\psi\Big|_0^{e^-}-EI\frac{\partial\psi}{\partial x}\delta\psi\Big|_{e^+}^{L}-kAG\left(\frac{\partial w}{\partial x}-\psi\right)\delta w\Big|_0^{e^-}\\&-kAG\left(\frac{\partial w}{\partial x}-\psi\right)\delta w\Big|_{e^+}^{L}-K_c\left(\left.\frac{\partial w}{\partial x}\right|_{e^+}-\left.\frac{\partial w}{\partial x}\right|_{e^-}\right)\delta\psi(t,e)\\&+\int_0^{e^-}\left[\frac{\partial}{\partial x}\left(EI\frac{\partial\psi}{\partial x}\right)+kAG\left(\frac{\partial w}{\partial x}-\psi\right)-\rho I\frac{\partial^2\psi}{\partial t^2}\right]\delta\psi\,dx\\&+\int_0^{e^-}\left[\frac{\partial}{\partial x}\left(kAG\left(\frac{\partial w}{\partial x}-\psi\right)\right)-\rho A\frac{\partial^2 w}{\partial t^2}\right]\delta w dx\\&+\int_{e^+}^{L}\left[\frac{\partial}{\partial x}\left(EI\frac{\partial\psi}{\partial x}\right)+kAG\left(\frac{\partial w}{\partial x}-\psi\right)-\rho I\frac{\partial^2\psi}{\partial t^2}\right]\delta\phi\,dx\\&+\int_{e^+}^{L}\left[\frac{\partial}{\partial x}\left(kAG\left(\frac{\partial w}{\partial x}-\psi\right)\right)-\rho A\frac{\partial^2 w}{\partial t^2}\right]\delta w dx\Bigg\}dt=0\end{aligned} \tag{4}$$

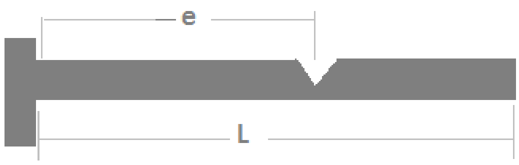

Figure 1. Timoshenko beam with a single-sided open crack.

For continuity of solution at location of the crack, it is necessary to have:

$$\begin{aligned}&\boldsymbol{w}(t,e^+)=w(t,e^-)=w(t,e)\\&\psi(t,e^+)=\psi(t,e^-)=\psi(t,e)\end{aligned} \tag{5}$$

then,

$$\begin{aligned}\int_{t_1}^{t_2}\Bigg\{&\left(\left[EI\frac{\partial\psi}{\partial x}\right]^{e^+}-\left[EI\frac{\partial\psi}{\partial x}\right]^{e^-}\right)\delta\psi(t,e)\\&-K_c\left(\left.\frac{\partial w}{\partial x}\right|_{e^+}-\left.\frac{\partial w}{\partial x}\right|_{e^-}\right)\delta\psi(t,e)+EI\frac{\partial\psi}{\partial x}\delta\psi\Big|_0\\&-EI\frac{\partial\psi}{\partial x}\delta\psi\Big|^{L}+kAG\left(\frac{\partial w}{\partial x}-\psi\right)\delta w\Big|_0-kAG\left(\frac{\partial w}{\partial x}-\psi\right)\delta w\Big|^{L}\\&+\left(\left[kAG\left(\frac{\partial w}{\partial x}-\psi\right)\right]^{e^+}-\left[kAG\left(\frac{\partial w}{\partial x}-\psi\right)\right]^{e^-}\right)\delta w(t,e)\\&+\int_0^{e^-}\left[\frac{\partial}{\partial x}\left(EI\frac{\partial\psi}{\partial x}\right)+kAG\left(\frac{\partial w}{\partial x}-\psi\right)-\rho I\frac{\partial^2\psi}{\partial t^2}\right]\delta\psi\\&+\int_0^{e^-}\left[\frac{\partial}{\partial x}\left(kAG\left(\frac{\partial w}{\partial x}-\psi\right)\right)-\rho A\frac{\partial^2 w}{\partial t^2}\right]\delta w dx\\&+\int_{e^+}^{L}\left[\frac{\partial}{\partial x}\left(EI\frac{\partial\psi}{\partial x}\right)+kAG\left(\frac{\partial w}{\partial x}-\psi\right)-\rho I\frac{\partial^2\psi}{\partial t^2}\right]\delta\phi dx\\&+\int_{e^+}^{L}\left[\frac{\partial}{\partial x}\left(kAG\left(\frac{\partial w}{\partial x}-\psi\right)\right)-\rho A\frac{\partial^2 w}{\partial t^2}\right]\delta w dx\Bigg\}dt=0\end{aligned} \tag{6}$$

Equation (6) gives the differential equations of motion and boundary conditions for w and ψ governed on two segments of the beam as follows:

For $0\le x<e$

$$\begin{aligned}&\boldsymbol{\rho A}\frac{\partial^2 w}{\partial t^2}-\frac{\partial}{\partial x}\left(kAG\left(\frac{\partial w}{\partial x}-\psi\right)\right)=0\\&\boldsymbol{\rho I}\frac{\partial^2\psi}{\partial t^2}-\frac{\partial}{\partial x}\left(EI\frac{\partial\psi}{\partial x}\right)-kAG\left(\frac{\partial w}{\partial x}-\psi\right)=0\\&EI\frac{\partial\psi}{\partial x}\delta\psi\Big|_0=0,\ kAG\left(\frac{\partial w}{\partial x}-\psi\right)\delta w\Big|_0=0\end{aligned} \tag{7}$$

and for $e<x\le L$

$$\begin{aligned}&\boldsymbol{\rho A}\frac{\partial^2 w}{\partial t^2}-\frac{\partial}{\partial x}\left(kAG\left(\frac{\partial w}{\partial x}-\psi\right)\right)=0\\&\boldsymbol{\rho I}\frac{\partial^2\psi}{\partial t^2}-\frac{\partial}{\partial x}\left(EI\frac{\partial\psi}{\partial x}\right)-kAG\left(\frac{\partial w}{\partial x}-\psi\right)=0\\&EI\frac{\partial\psi}{\partial x}\delta\psi\Big|^{L}=0,\ kAG\left(\frac{\partial w}{\partial x}-\psi\right)\delta w\Big|^{L}=0\end{aligned} \tag{8}$$

Also, at crack location:

$$\begin{aligned}&\boldsymbol{w}(t,e^+)=w(t,e^-)\\&EI\left.\frac{\partial\psi}{\partial x}\right|_{e^+}-EI\left.\frac{\partial\psi}{\partial x}\right|_{e^-}=K_c\left(\left.\frac{\partial w}{\partial x}\right|_{e^+}-\left.\frac{\partial w}{\partial x}\right|_{e^-}\right)\\&\left[kAG\left(\frac{\partial w}{\partial x}-\psi\right)\right]^{e^+}-\left[kAG\left(\frac{\partial w}{\partial x}-\psi\right)\right]^{e^-}=0\end{aligned} \tag{9}$$

Introducing the following non-dimensional quantities:

$$\xi=\frac{x}{L},\ \vartheta=\frac{kG}{E},\ r=\frac{AL^2}{I},\ s=\vartheta r,\ \tau=\sqrt{\frac{EI}{\rho AL^4}}t,\ \eta=\frac{w}{L} \tag{10}$$

Substituting the above dimensionless quantities in Equations (7) and (8) gives:

$$\begin{aligned}&\frac{\partial^2\eta}{\partial\tau^2}-s\frac{\partial^2\eta}{\partial\xi^2}+s\frac{\partial\psi}{\partial\xi}=0\\&\frac{\partial^2\psi}{\partial\tau^2}-r\frac{\partial^2\psi}{\partial\xi^2}+sr\psi-sr\frac{\partial\eta}{\partial\xi}=0\end{aligned} \tag{11}$$

Assuming a harmonic solution in the following form:

$$\begin{Bmatrix}\eta(\tau,\xi)\\ \psi(\tau,\xi)\end{Bmatrix}=\begin{Bmatrix}\mathrm{X}(\xi)\\ \Psi(\xi)\end{Bmatrix}e^{i\bar{\omega}\tau} \tag{12}$$

in which $\bar{\omega}$ is dimensionless natural frequency. Obtaining $\Psi(\xi)$ in terms of $\mathrm{X}(\xi)$ gives:

$$\frac{d^4\mathrm{X}}{d\xi^4}+\bar{\omega}^2\left(\frac{1}{r}+\frac{1}{s}\right)\frac{d^2\mathrm{X}}{d\xi^2}+\bar{\omega}^2\left(\frac{\bar{\omega}^2}{sr}-1\right)\mathrm{X}=0 \tag{13}$$

Assuming a solution in the following form:

$$\mathbf{X}=Ae^{\lambda\xi} \tag{14}$$

The characteristic equation for determining the eigenvalue of λ will be obtained as:

$$\lambda^4+\bar{\omega}^2\left(\frac{1}{\mathrm{r}}+\frac{1}{s}\right)\lambda^2+\bar{\omega}^2\left(\frac{\bar{\omega}^2}{\mathrm{sr}}-1\right)=0 \tag{15}$$

from which:

$$\begin{aligned}&\lambda_1=\sqrt{\bar{\omega}\sqrt{\frac{\bar{\omega}^2}{4}\left(\frac{1}{\mathrm{r}}-\frac{1}{\mathrm{s}}\right)^2+1}-\frac{\bar{\omega}^2}{2}\left(\frac{1}{\mathrm{r}}+\frac{1}{s}\right)}\\&\lambda_2=\sqrt{\bar{\omega}\sqrt{\frac{\bar{\omega}^2}{4}\left(\frac{1}{\mathrm{r}}-\frac{1}{\mathrm{s}}\right)^2+1}+\frac{\bar{\omega}^2}{2}\left(\frac{1}{\mathrm{r}}+\frac{1}{s}\right)}\end{aligned} \tag{16}$$

then

$$\begin{aligned}&\mathbf{X}(\xi)=C_1\cosh\lambda_1\xi+C_2\sinh\lambda_1\xi+C_3\cos\lambda_2\xi+C_4\sin\lambda_2\xi\\&\mathbf{\Psi}(\xi)=C_1\left(\frac{\bar{\omega}^2}{s\lambda_1}+\lambda_1\right)\sinh\lambda_1\xi+C_2\left(\frac{\bar{\omega}^2}{s\lambda_1}+\lambda_1\right)\cosh\lambda_1\xi\\&+C_3\left(\frac{\bar{\omega}^2}{s\lambda_2}-\lambda_2\right)\times\sin\lambda_2\xi-C_4\left(\frac{\bar{\omega}^2}{s\lambda_2}-\lambda_2\right)\cos\lambda_2\xi\end{aligned} \tag{17}$$

Accordingly, the boundary conditions will be:

$$\begin{aligned}&\mathrm{X}_1(e)=\mathrm{X}_2(e),\\&\frac{d\mathrm{X}_2(e)}{d\xi}-\frac{d\mathrm{X}_1(e)}{d\xi}-\frac{1}{K_{cb}}\frac{d\Phi_1(e)}{d\xi}=0\\&\frac{d\Phi_2(e)}{d\xi}-\frac{d\Phi_1(e)}{d\xi}=0,\\&\frac{d\mathrm{X}_2(e)}{d\xi}-\frac{d\mathrm{X}_1(e)}{d\xi}-\Phi_2(e)+\Phi_1(e)=0\end{aligned} \tag{18}$$

where

$$K_{cb}=\frac{L}{6h\pi\ f_j(\eta)} \tag{19}$$

The cracked section may be modelled as a local flexibility in order to study the effects of the crack. In this manner the crack is regarded as a rotational spring. The discontinuity in the slope of beam at the cracked section may be implemented as done in ([24]). Equating the structural bending moment of two sides of the crack with the bending moment due to crack which is modelled by rotational stiffness of K_c, gives:

$$\boldsymbol{EI}\frac{\partial\phi}{\partial x}=K_c\left(\left.\frac{\partial w}{\partial x}\right|_{e^+}-\left.\frac{\partial w}{\partial x}\right|_{e^-}\right) \tag{20}$$

where K_c is the rotational stiffness and is given by [24] as follows:

$$K_c=\frac{bh^2E}{72\pi\ f_j(\eta)} \tag{21}$$

In Equation (19), K_{cb} is the dimensionless crack sectional flexibility and depends on the extension of the crack. The equation of a single-sided open crack may be written [25] as:

$$\begin{aligned}&f_j(\eta)=0.6384\eta^2-1.035\eta^3+3.7201\eta^4-5.1773\eta^5\\&+7.553\eta^6-7.332\eta^7+2.4909\eta^8\end{aligned} \tag{22}$$

in which, η is a dimensionless crack-depth ratio with $\eta=a/h$.

3. BACK-PROPAGATION NEURAL NETWORK

Back-propagation neural network is a well-established method to multiple-layer networks and nonlinear differentiable transfer functions. Input vectors and the corresponding target vectors are used to train a network. The trained network should be capable of approximating a function, also, associate input vectors with specific output vectors, as well as classifying input vectors in an appropriate way. Properly trained Back-propagation networks tend to give reasonable answers when presented with inputs which have been never seen. The general structure of this network is shown in Figure 2.

To simulate the network, a static network (a network with no delay and no feedback) is required. Also, since the network needs to be trained with different examples, a supervised network is required. It means that the network needs examples of target which is related to input (input/target pairs) to understand the ruling regularity of the network. Back-propagation is a static, supervised [26] neural network. This network has a great performance regardless of increasing or decreasing of the data. There is such datum regarding this study. For example, in a special crack location, natural frequencies decrease as the crack depth increases. This network, also, makes a balance between memorization and generalization. All these characteristics lead us to use Back-propagation among different types of neural networks to find out the location and depth of the crack.

Since the errors are fed backward in the network to correct the weights and again the input repeats the path to the output in the network, the term "Back-propagation" has been used. The amounts of the weights of the network are supposed to be determined randomly. In each step, the output is calculated and the weights are corrected according to their difference with the desired output. Assume that w_{ji} is the weight between the input layer and the hidden one. Therefore:

$$A_j\left(\bar{x},\bar{w}\right)=\sum_{i=0}^{\infty} x_i w_{ji} \tag{23}$$

Assuming the output function as sigmoid $sgm(x) = 1/(1+e^{-x})$ the output of the jth neuron will be as:

$$O_j\left(\bar{x},\bar{w}\right)=\mathrm{sgm}\left(A_j\left(\bar{x},\bar{w}\right)\right)=\frac{1}{1+e^{-A_j\left(\bar{x},\bar{w}\right)}} \tag{24}$$

An study on the above equation reveals that any change in the weights causes the output to be changed. To achieve the desired output, error function of each neuron should be calculated as follows:

$$E_j\left(\bar{x},\bar{w}\right)=\left(O_j\left(\bar{x},\bar{w}\right)-d_j\right)^2 \tag{25}$$

where O_j is the real output and d_j is the desired output. Therefore, the total error of the network will be the sum of the error of each neuron. So,

$$\boldsymbol{E}\left(\bar{x},\bar{w},d\right)=\sum E_j\left(\bar{x},\bar{w},d_j\right) \tag{26}$$

The relation between error and input, also, between error and output as well as between error and weights need to be considered. The purpose is to change the weights in order to minimize the error function. There are different methods to achieve this goal. Standard Back-propagation neural network uses a gradient descent algorithm. According to the parabolic and positive behaviour of the error function, it is required to move along the negative path of the gradient of the function to achieve the minimum amount of the error.

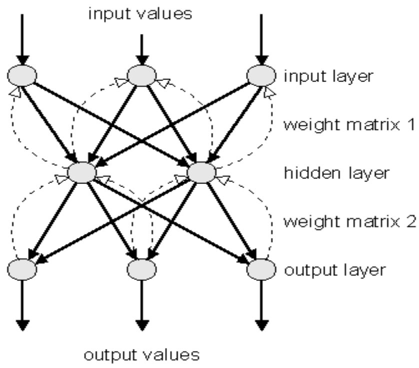

Figure 2. The general structure of a Back-propagation neural network with 3 layers.

Therefore, the gradient of the error function with respect to weights is necessary to be computed. The weights should be changed in such a way that the error become minimize. After some simple manipulations, the change in weights is given by the following formula:

$$\boldsymbol{\Delta} w_{ji}=-\eta_1\frac{\partial E}{\partial w_{ji}}=-2\eta_1\left(O_j-d_j\right)O_j\left(1-O_j\right)x_i \tag{27}$$

where η_1 is a selective constant to modify the weights.

The above formula is used for modifying the weights of a network consisting of two layers (input-output). Supposing a hidden layer, two kinds of weights are needed to be modified on each step in the Back-propagation neural network algorithm i.e., weights that relate the input layer to the hidden one, $\bar{v}$, and weights which relate the hidden layer to output layer, $\bar{w}$. Under this condition, the error depends on both v_{jk} and the weights that relate the hidden layer to the output layer, w_{ji}. Using the gradient descent algorithm and the same process, $\boldsymbol{\Delta} v_{jk}$ is:

$$\boldsymbol{\Delta} v_{ji}=-\eta_1\frac{\partial E}{\partial v_{jk}}=-\eta_1\frac{\partial E}{\partial x_i}x_iO_j\left(1-x_i\right)v_{jk} \tag{28}$$

In a 3 layer network, the input of the output layer is output of the hidden layer, therefore:

$$\frac{\partial E}{\partial w_{ji}}=2\left(O_j-d_j\right)O_j\left(1-O_j\right)w_{ji} \tag{29}$$

Some input and output patterns can be easily learned by single-layer neural networks. However, these single-layer neural networks cannot learn some relatively simple patterns, since those are not linearly separable. A multi-layered network overcomes this limitation, since, it can create internal features and learn each layer. Each prior layer learns more abstract features. Each layer finds patterns in its below layer. Creation of internal features that are independent of input is the power of the Back-propagation neural network. The goal and motivation for developing the Back-propagation algorithm is to find out a way to train multi-layered neural networks such that it can create the appropriate internal features to allow it to learn any arbitrary mapping of input to output. It can be proved that a Back-propagation neural network with more than 3 layers has an efficiency close to a 3-layer network. Therefore, use of a Back-propagation neural network with more than three layers does not have remarkable efficiency rather than a three layer one. On the other hand, it takes much more time and CPU usage. So, it is common to use a 3-layer Back-propagation neural network. Complete discussion can be observed in [26].

4. PROCEDURE OF IDENTIFYING THE CRACK BY NEURAL NETWORK

The natural frequencies of the cracked beam are directly determined through solving the equation of the cracked beam. An inverse problem makes use the known natural frequencies to obtain the crack location x/L or l_1 and crack depth a/H or η. Indeed, in an inverse problem, we try to find out the unknown parameters of the problem by both the measured natural frequencies and the other properties of the structure. In this problem, the unknown parameters are the location and depth of the crack. The term ω_i/ω_n is defined as the dimensionless natural frequency where ω_i is the *i*th natural frequency of the cracked beam of length L and ω_{in} is the *i*th natural frequency of intact beam of the same length. To determine the location and depth of the crack by neural network, a lot of examples should be provided for training the neural network. With the known l_1 and η, as well as boundary conditions, one can obtain the natural frequencies of the cracked beam. In this method, the first four natural frequencies are obtained for different crack locations and depths. At the next step, this data is used for training the neural network.

In current work, the cracked beam models are assumed to be made of mild steel with the following material properties: Young's modulus $E = 210\,\mathrm{GPa}$, material mass density $\rho = 7860\,\mathrm{kg/m^3}$ and Poisson's ratio $\nu = 0.3$. The value of the Timoshenko shear coefficient k' for the rectangular cross-section of the present research is taken as 5/6. The geometric data of the beam are: beam depth $H = 25\,\mathrm{mm}$, beam thickness $B = 12.5\,\mathrm{mm}$ and beam length $L = 125\,\mathrm{mm}$ [15]. The natural frequency of the cracked beam is a function of l_1 (dimensionless crack location) and θ; crack sectional flexibility which is function of η (dimensionless crack depth). For providing examples to train the neural network, the first four natural frequencies may be obtained by solving the Equations (17), (18) along with applying the boundary conditions according to different crack location and depth. For this purpose, l_1 and η are changed from 0 to 1 by a specific step. Then, the first four natural frequencies related to each pair of l_1 and η are obtained. Here, l_1 is changed from 0.05 to 0.95 by step 0.015 (61 conditions). Simultaneously, η is changed from 0.1 to 0.91 by step 0.015 (55 conditions) and the dimensionless natural frequencies are obtained. This operation made $61 \times 55 = 3355$ pairs of dimensionless crack location and depth with related natural frequencies. They are used for training the neural network. Solving the problem inversely (using natural frequencies in order to determine the crack location and depth), the dimensionless frequencies are given as input layer and crack location and depth are given as output layer to the network.

5. RESULTS AND DISCUSSION

5. 1. Validity of Equation of Motion In this section, we study the validity of presented equation of motion. For this purpose, the first three natural frequencies of the beam with different boundary conditions are calculated. These results have been compared with those presented by Khaji et al. [15]. Both the results i.e. results of this study and those of [15] are presented in Table 1 in order to make a comparison between them. It is clear that there are very good conformity between these two sets of results. Also, some of the results that show the changes in natural frequencies due to the effect of varying the parameters of the beam are presented in this table. The first three natural mode shapes of the beam with different boundary conditions are shown if Figures 3a, 3b and 3c. These figures make clear that the slope experiences the change when there is not any node in the mid of the beams for different boundary condition. Now after presenting the validity of equations of motions, the necessary data for training the neural network is prepared. These data will be obtained according to [15].

5. 2. Prediction of Crack Location in a Beam with Different Boundary Conditions Training the neural network was performed in three conditions: condition 1: with 3 dimensionless frequencies as input, condition 2: with 4 dimensionless frequencies as input and condition 3: with 5 dimensionless frequencies as input.

TABLE 1. Comparison of the three first natural frequency of cracked Euler-Bernoulli beam models for various boundary conditions ($L=100\mathbf{mm}, L/h=4, e=0.5$)

Boundary conditions	Dimensionless crack depth ratio $\eta=a/h$	$f_1(Hz)$		$f_2(Hz)$		$f_3(Hz)$	
		Ref. [15]	Present work	Ref. [15]	Present work	Ref. [15]	Present work
Simply supported	0.2	4911.8	4911.85099	17,603.8	17,603.7887	30,952.5	30,952.57562
	0.3		4474.18306		17,603.7887		29,679.53566
	0.4		3956.26216		17,603.7887		28,414.2587
Simple-clamped	0.2	7139.0	7139.0115	19,600.2	19,600.1452	32,236.1	32,236.1366
	0.3		6787.02786		19,570.45638		30,938.0554
	0.4		6390.63396		19,535.74335		29,659.60941
Clamped-clamped	0.2	9408.6	9408.6129	21,397.5	21,397.5208	33,378.1	33,378.1168
	0.3		9054.879		21,397.5208		32,006.0543
	0.4		8663.457		21,397.5208		30,660.9051
Simple-free-shear	0.2	1361.7	1361.66519	10,575.5	10,575.48692	24,196.6	24,196.612137
	0.3		1286.136444		10,192.12776		23,6104.79146
	0.4		1185.84391		9,7587.108628		23,009.23042
Clamped-free-shear	0.2	3007.7	3007.69978	12,697.3	12,697.2838	26,038.2	26,038.15901
	0.3		3002.53633		12,197.9082		25,594.80291
	0.4		2996.15096		11,642.40153		25,136.41062
Cantilever beam	0.2	1948.2	1948.205	9393.7	9393.6829	22,962.3	22,962.30567
	0.3		1893.79564		8722.531		22,859.6366
	0.4		1812.83689		7974.77909		22748.2826

Back-propagation neural network is selected to determine crack location and depth. As mentioned, the input layer contains 3, 4 or 5 neurons which include condition 1 (training with 3 dimensionless frequencies) , 2 (training with 4 dimensionless frequencies) or 3 (training with 5 dimensionless frequencies) and the output layer contains 2 neurons which includes crack location and depth. 70 neurons were selected to be in the hidden layer (middle layer). Because of the existence of the symmetry in the beam, the number of epochs was chosen 2500 for simply-supported and clamped-clamped boundary conditions. On the other hand, the number of epochs was 3000 due to the asymmetric property of the cantilever beam. Convergence of the number of neurons in hidden layer and epochs were tested by choosing different number of neurons and epochs. Besides, Bayesian algorithm was used to train the neural network.

5. 2. 1. Determination of Crack Location in a Simply Supported Beam Due to the symmetry of the beam, half of its length is considered and analysed, namely, $0 \le (l_1 = x/L) \le 0.5$. So, a number of $31\times 55=1705$ pairs of crack location and depth with the related natural frequencies are used to train the neural network. The dimensionless natural frequency ω_4/ω_{4n} for three selective crack depths (η) is shown in Figure 4. The term ω_3/ω_{3n} is related to training neural network with the first three dimensionless frequencies (condition 1), ω_4/ω_{4n} is related to training neural network with the first four dimensionless frequencies (condition 2) and ω_5/ω_{5n} is related to training neural network with the first three dimensionless frequencies (condition 3). Figures 5, 6 and 7 show the error percentage in prediction of the crack location by the neural network. Firstly, as may be seen, the more distance from the boundary conditions, the less will be the errors. Furthermore, the maximum error for condition 1 (training with 3 frequencies), is about 10 percent, while the error for condition 2 (training with 4 frequencies) and condition 3 (training with 5 frequencies) is about 4 and 3 percent, respectively. It means that using more natural frequencies to train the neural network make the error to be decreased more.

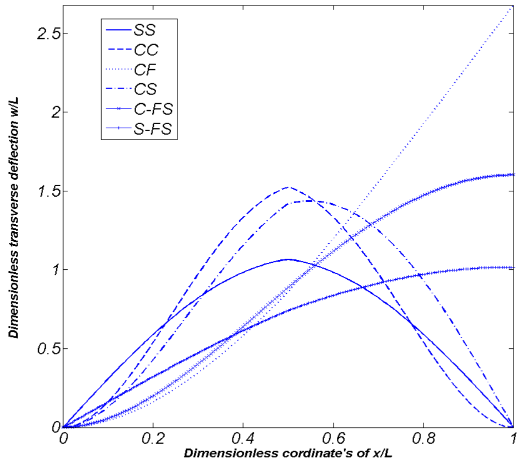

(a)

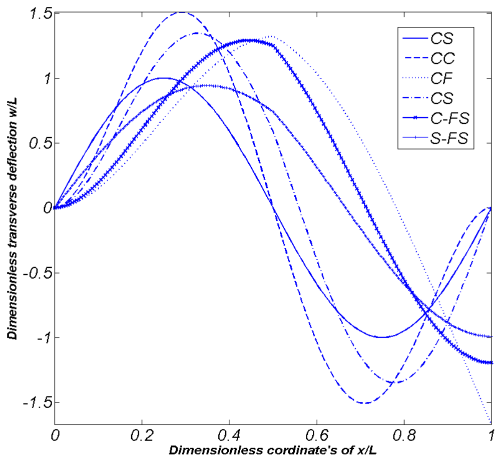

(b)

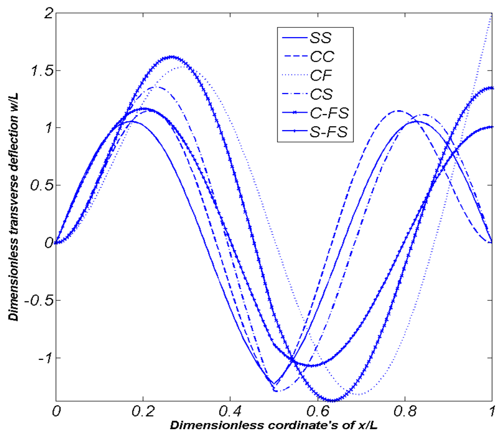

(c)

Figure 3. The first three mode shapes of beams with different boundary conditions a) first mode shape, b) second mode shape and c) third mode shape (SS- simply-simply, CC: clamped-clamped, CF: clamped-free, CS: clamped-simply, C-FS: clamped-free sliding, S-FS: clamped-free sliding).

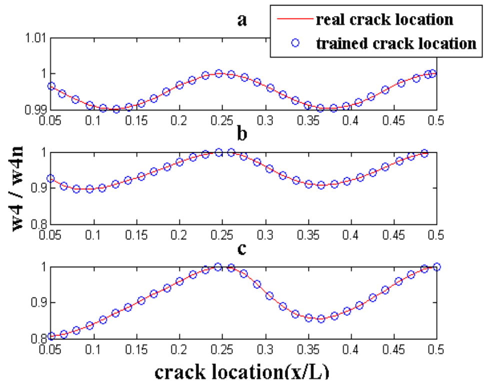

Figure 4. ω_4/ω_{4n} versus crack location in three selective crack depths: a) $\eta = 0.1$, b) $\eta = 0.4$, c) $\eta = 0.7$.

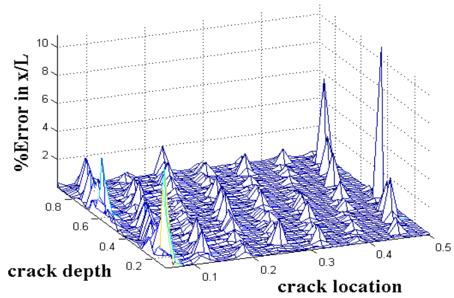

Figure 5. Percent of error in crack location of a simply-supported beam for condition 1(training with 3 frequencies).

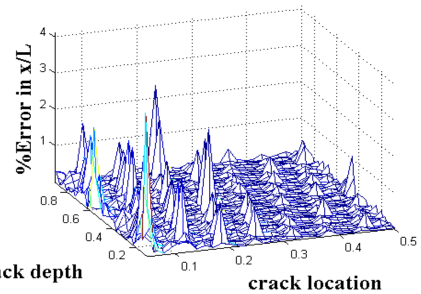

Figure 6. Percent of error in crack location of a simply-supported beam for condition 2 (training with 4 frequencies).

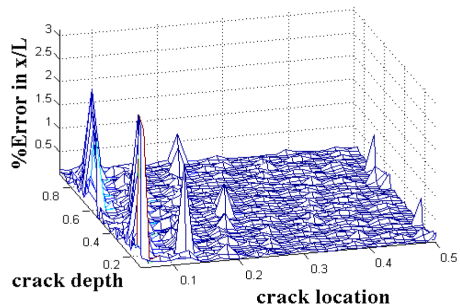

Figure 7. Percent of error in crack location of a simply-supported beam for condition 3 (training with 5 frequencies).

Figure 8 shows the performance plot of the network for a simply-supported beam for condition 2 (training with 4 frequencies) for $\eta = 0.1$. However, due to the low differences in errors, the performance plots of the network for different boundary conditions are similar in conditions 1, 2 and 3.

If the step of changing l_1 is chosen 0.02 instead of 0.015, there are $31 \times 41 = 1271$ pairs of dimensionless crack location and depth with related natural frequencies. Also, if both l_1 and η are changed by step 0.02 instead of 0.015, there are $23 \times 41 = 943$ pairs. These errors (1271 pairs and 943 pairs) for a simply-supported beam for condition 2 (training with 4 frequencies) are shown in Figures 9 and 10, respectively. The error percentage for training with 1271 and 943 pairs is about 6 and 14 percent, respectively, while the maximum error corresponding to 1705 pairs is about 4 percent. If the errors more than 6 percent not to be acceptable, one can conclude that the step of length 0.015 is good and reliable.

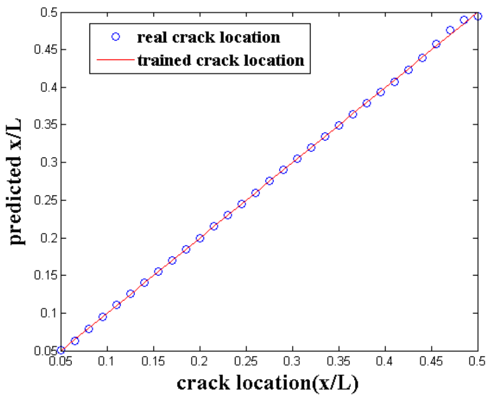

Figure 8. Performance plot of the network for a simply-supported beam for condition 2 (training with 4 frequencies) in $\eta = 0.1$.

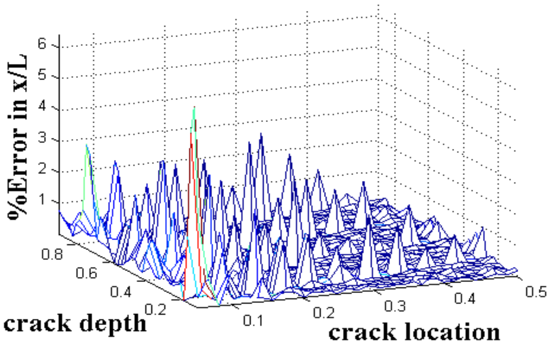

Figure 9. Percent error in crack location of a simply-supported beam for condition 2 (training with 4 frequencies), for the combination of $31 \times 41 = 1271$ pairs.

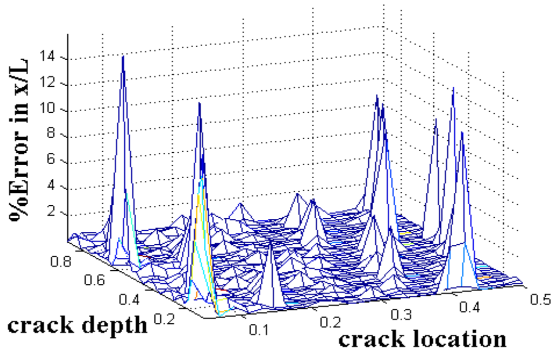

Figure 10. Percent error in crack location of a simply-supported beam for condition 2 (training with 4 frequencies), for the combination of $23 \times 41 = 943$ pairs.

5. 2. 2. Determination of Crack Location in a Clamped-clamped Beam The location and depth of the crack in the clamped-clamped beam may be determined in the same manner as applied on a simply-supported beam, previously. In simply-supported beam, it was mentioned that an increase in the number of the dimensionless frequencies to train the neural network, makes the prediction error to be decreased. It is also true for a beam with any other boundary conditions. Because of the symmetry, half of the beam is considered. In this case, Figure 11 shows the error percentage in crack location of this beam in conditions 2 (training with 4 frequencies).

5. 2. 3. Determination of Crack Location in a Cantilever Beam In this case, the number of provided examples to train the neural network is 3355 because whole length of the beam is considered. Figure 12 shows error percentage of the neural network in crack location prediction of a cantilever beam for condition 2 (training with 4 frequencies).

5. 3. Prediction of Crack Depth in Different Boundary Conditions Here, the capability of the proposed neural network for prediction of the crack depth of the beams with different boundary conditions is investigated. The error percentage of the prediction of the crack depth of a simply-supported, clamped-clamped and cantilever beam for condition 2 (training with 4 frequencies) are shown in Figures 13, 14 and 15, respectively. For better understanding of the error in prediction of the location and depth of a crack simply-supported beam of condition 2 (training with 4 frequencies) has been studied. In this study a number of random frequencies have been used. The error percentages between real and predicted location and depth of the crack are computed and along with the random frequencies are presented in Tabel 2.

TABEL 2. Some random first four frequencies given to the network and computing errors.

First four dimensionless frequencies	Real		Predicted		Error percentage	
	Crack depth	Crack location	Crack depth	Crack location	Crack depth	Crack location
0.977859785 0.998238588 0.988428635 0.995997529	2.75 (0.11)	6.875 (0.55)	2.8047 (0.1122)	6.9258 (0.546)	1.99%	0.07%
0.595446392 0.659468287 0.861820767 0.96928069	20.75 (0.83)	26.25 (0.21)	20.7557 (0.8298)	26.252 (0.21)	0.03%	0.01%
0.57859434 0.848450939 0.984904873 0.859121407	16.25 (0.65)	45 (0.36)	16.259 (0.6504)	45.0701 (0.3606)	0.06%	0.16%
0.819637274 0.986317317 0.917921335 0.973222096	8.75 (0.35)	56.25 (0.45)	8.7533 (0.3499)	56.2555 (0.45)	0.04%	0.01%

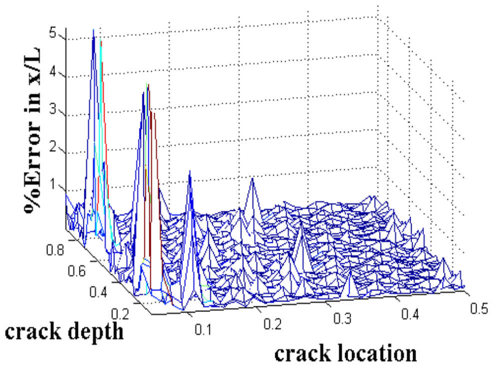

Figure 11. Percent error in crack location of a clamped-clamped beam for condition 2.

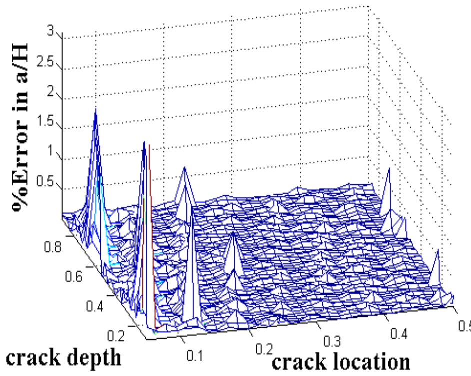

Figure 13. Percent error in crack depth of a simply-supported beam for condition 2.

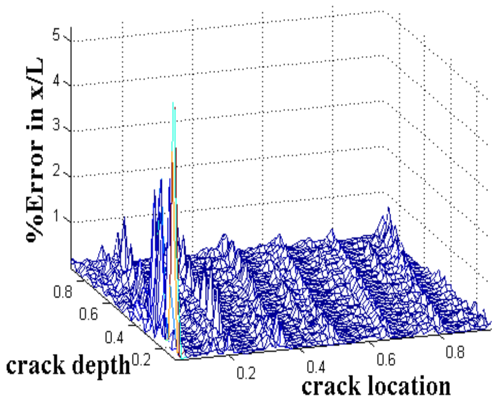

Figure 12. Percent error in crack location of a cantilever beam for condition 2.

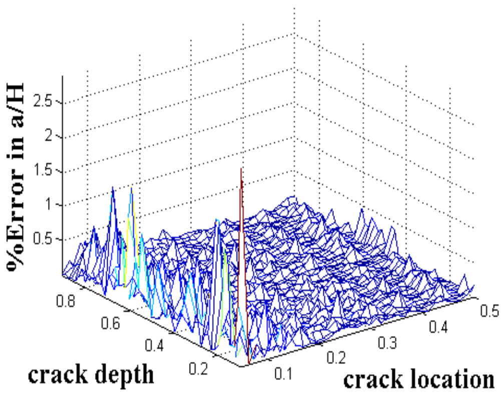

Figure 14. Percent error in crack depth of a clamped-clamped beam for condition 2.

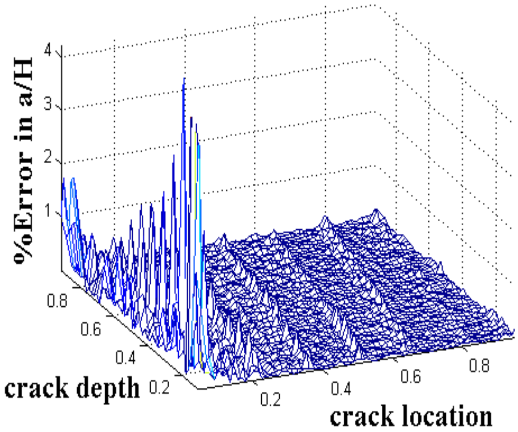

Figure 15. Percent error in crack depth of a cantilever beam for condition 2.

6. UNIQUENESS OF THE CRACK LOCATION AND DEPTH

The process of the prediction of the location and depth of a crack by the neural network or application of vibrational data in an inverse problem conducted a good feature. This feature is the uniqueness of the obtained data in the inverse problem. This feature makes ensure that the neural network can exactly determine the location and depth of the crack. Here there is a question; if the different cracks with different location and depth may result in similar natural frequencies? This similarity may take place for the first and second natural frequencies of the cracks at different location and depth, but for the next natural frequencies, such as their third, fourth and other natural frequencies the similarity will not happen. Hence, using more than two natural frequencies, the uniqueness of the answer will be satisfied. However, the uniqueness of the answer when using the first or the first two dimensionless frequencies has not been guaranteed.

7. CONCLUDING REMARKS

In this research, the location and depth of the crack of a beam are obtained by neural network. According to the results, it is shown that the neural network is a trustable and powerful method to obtain the crack location and depth. Also, the results show that, increasing the number of natural frequencies to train the neural network causes the errors to be reduced. It means, obtaining more accurate results implies using more number of natural frequency to train the neural network.

8. REFERENCES

.

1. Babot, D., Berodias, G. and Peix, G., "Detection and sizing by x-ray compton scattering of near-surface cracks under weld deposited cladding", ***NDT & E International***, Vol. 24, No. 5, (1991), 247-251.
2. Taghi, M., Baghmishehe, V., Peimani, Sadeghi, M. H., and Ettefagh, M. M "Crack detection in beam-like structures using genetic algorithms", ***Applied Soft Computing***, Vol. 8, No. 2, (2008), 1150-1160.
3. Nahvi, H. and Jabbari, M., "Crack detection in beams using experimental modal data and finite element model", ***International Journal of Mechanical Sciences***, Vol. 47, No. 10, (2005), 1477-1497.
4. Nandwana, B. and Maiti, S., "Modelling of vibration of beam in presence of inclined edge or internal crack for its possible detection based on frequency measurements", ***Engineering Fracture Mechanics***, Vol. 58, No. 3, (1997), 193-205.
5. Zhong, S. and Oyadiji, S. O., "Crack detection in simply supported beams without baseline modal parameters by stationary wavelet transform", ***Mechanical Systems and Signal Processing***, Vol. 21, No. 4, (2007), 1853-1884.
6. Rizos, P., Aspragathos, N. and Dimarogonas, A., "Identification of crack location and magnitude in a cantilever beam from the vibration modes", ***Journal of Sound and Vibration***, Vol. 138, No. 3, (1990), 381-388.
7. Chondros, T. G. and Dimarogonas, A. D., "Influence of a crack on the dynamic characteristics of structures", ***Journal of Vibration, Acoustics, Stress and Reliability in Design***, Vol. 111, (1989), 251-256.
8. Adams, R., Cawley, P., Pye, C. and Stone, B., "A vibration technique for non-destructively assessing the integrity of structures", ***Journal of Mechanical Engineering Science***, Vol. 20, No. 2, (1978), 93-100.
9. Gudmundson, P., "The dynamic behaviour of slender structures with cross-sectional cracks", ***Journal of the Mechanics and Physics of Solids***, Vol. 31, No. 4, (1983), 329-345.
10. Liang, R. Y., Hu, J. and Choy, F., "Theoretical study of crack-induced eigenfrequency changes on beam structures", ***Journal of Engineering Mechanics***, Vol. 118, No. 2, (1992), 384-396.
11. Fernandez-Saez, J. and Navarro, C., "Fundamental frequency of cracked beams in bending vibrations: An analytical approach", ***Journal of Sound and Vibration***, Vol. 256, No. 1, (2002), 17-31.
12. Lele, S. and Maiti, S., "Modelling of transverse vibration of short beams for crack detection and measurement of crack extension", ***Journal of sound and Vibration***, Vol. 257, No. 3, (2002), 559-583.
13. Orhan, S., "Analysis of free and forced vibration of a cracked cantilever beam", ***NDT & E International***, Vol. 40, No. 6, (2007), 443-450.
14. Shafiei, M. and Khaji, N., "Analytical solutions for free and forced vibrations of a multiple cracked timoshenko beam subject to a concentrated moving load", ***Acta Mechanica***, Vol. 221, No. 1-2, (2011), 79-97.
15. Khaji, N., Shafiei, M. and Jalalpour, M., "Closed-form solutions for crack detection problem of timoshenko beams with various boundary conditions", ***International Journal of Mechanical Sciences***, Vol. 51, No. 9, (2009), 667-681.
16. Yan, T., Kitipornchai, S., Yang, J. and He, X. Q., "Dynamic behaviour of edge-cracked shear deformable functionally graded beams on an elastic foundation under a moving load", ***Composite Structures***, Vol. 93, No. 11, (2011), 2992-3001.

17. Matbuly, M., Ragb, O. and Nassar, M., "Natural frequencies of a functionally graded cracked beam using the differential quadrature method", ***Applied Mathematics and Computation***, Vol. 215, No. 6, (2009), 2307-2316.
18. Mazanoglu, K. and Sabuncu, M., "Vibration analysis of non-uniform beams having multiple edge cracks along the beam's height", ***International Journal of Mechanical Sciences***, Vol. 52, No. 3, (2010), 515-522.
19. Hadjileontiadis, L. J., Douka, E. and Trochidis, A., "Crack detection in beams using kurtosis", ***Computers & Structures***, Vol. 83, No. 12, (2005), 909-919.
20. Douka, E., Loutridis, S. and Trochidis, A., "Crack identification in beams using wavelet analysis", ***International Journal of Solids and Structures***, Vol. 40, No. 13, (2003), 3557-3569.
21. Lu, X., Liu, J. and Lu, Z., "A two-step approach for crack identification in beam", ***Journal of Sound and Vibration***, (2012).
22. Attar M., A. "A transfer matrix method for free vibration analysis and crack identification of stepped beams with multiple edge cracks and different boundary conditions", ***International Journal of Mechanical Sciences*** Vol. 57, (2012), 19-33.
23. Rao, S. S., "Vibration of continuous systems", John Wiley & Sons, (2007).
24. Haisty, B., Duerr, R. and Springer, W., "A general beam element for use in damage assessment of complex structures", in Advanced Technologies in Failure Prevention: Proceedings of the 43rd Meeting of the Mechanical Failures Prevention Group, Cambridge University Press. (1991), 145.
25. Ostachowicz, W. and Krawczuk, M., "Analysis of the effect of cracks on the natural frequencies of a cantilever beam", ***Journal of Sound and Vibration***, Vol. 150, No. 2, (1991), 191-201.
26. Haykin, S., "Neural networks: A comprehensive foundation", Prentice Hall PTR, (1994).

Crack Detection of Timoshenko Beams Using Vibration Behavior and Neural Network

M. Rakideh, M. Dardel, M. H. Pashaei

Babol Noshirvani University of Technology, Department of Mechanical Engineering, Babol, Iran

PAPER INFO

Paper history:
Received 27 January 2013
Received in revised form 12 March 2013
Accepted 18 April 2013

Keywords:
Crack Detection
Timoshenko Beam
Neural Network

چکیده

در این تحقیق ابتدا فرکانس‌های طبیعی تیر ترکدار به‌روش تحلیلی بدست آمده است. بدنبال آن موقعیت و عمق ترک در تیر با استفاده از روش شبکه عصبی تعیین گردیدند. این مطالعه بر روی یک تیر با یک ترک باز و در سه شرایط مرزی مختلف انجام گرفت. برای این منظور فرکانس‌های طبیعی تیر ترکدار در ابتدا به‌روش تحلیلی تعیین و برای آموزش شبکه عصبی بکار گرفته شدند. در ادامه و در عکس حالت قبل، شبکه عصبی آموزش دیده جهت تعیین موقعیت و عمق ترک مورد استفاده قرار گرفت. همچنین اثر تعداد فرکانس‌های طبیعی بعنوان ورودی شبکه عصبی روی دقت کار مورد ارزیابی قرارگرفت. نتایج بدست‌آمده و مقادیر خطا نشان میدهد که شبکه عصبی روشی توانمند در تعیین محل و عمق ترک در تیر می‌باشد. بعلاوه با افزایش تعداد فرکانس‌های طبیعی یا همان افزایش محدوده تحلیل دقت پیش‌بینی افزایش می‌یابد.

doi: *10.5829/idosi.ije.2013.26.12c.04*